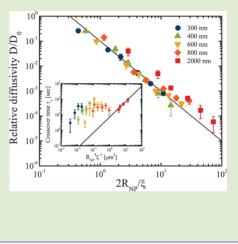# Size-Dependent Dynamics of Nanoparticles in Unentangled Polyelectrolyte Solutions

Ryan Poling-Skutvik, Ramanan Krishnamoorti,* and Jacinta C. Conrad*

Department of Chemical and Biomolecular Engineering, University of Houston, Houston, Texas 77204-4004, United States

S *Supporting Information*

ABSTRACT: The mobility of polystyrene nanoparticles ranging in diameter from 300 nm to 2 μm was measured in dilute and semidilute solutions of partially hydrolyzed polyacrylamide. In this model system, the ratio of particle to polymer size controls the long-time diffusivity of nanoparticles. The particle dynamics transition from subdiffusive on short time scales to Fickian on long time scales, qualitatively similar to predictions for polymer dynamics using a Rouse model. The diffusivities extracted from the long-time Fickian regime, however, are larger than those predicted by the Stokes−Einstein equation and the bulk zero-shear viscosity and moreover do not collapse according to hydrodynamic models. The size-dependent deviations of the long-time particle diffusivities derive instead from the coupling between the dynamics of the particle and the polymer over the length scale of the particle. Although the long-time diffusivities collapse according to predictions, deviations of the short-time scaling exponents and the crossover time between subdiffusive and Fickian dynamics indicate that the particles are only partially coupled to the relaxation modes of the polymer.

Transport of nanoparticles through non-Newtonian media affects applications ranging from targeted drug delivery[1,2] to oil recovery[3,4] to nanocomposite materials.[5,6] In a homogeneous medium of viscosity η, the diffusivity of a particle with radius R_{NP} is given by the Stokes−Einstein (SE) equation $D_{SE} = k_B T / 6 \pi \eta R_{NP}$. As particle size approaches characteristic length scales in the medium, the continuum assumption underlying the SE relation no longer holds, and deviations from SE predictions appear.[7−10] Attempts to explain these deviations in mixtures of polymers and particles have focused on identifying the length scale that controls particle diffusion.

In entangled polymer systems, the length scale controlling particle diffusion is the distance between entanglements. The diffusion of nanoparticles smaller than the entanglement mesh is unaffected by entanglement dynamics, but for larger particles diffusion is dictated by polymer reptation until SE behavior is recovered.[11−14] In unentangled systems, however, different physics must control nanoparticle diffusion. Hydrodynamic models treat the polymer solution as a homogeneous medium in which hydrodynamic interactions are screened over the correlation length between polymer chains ξ.[10,15,16] Scaling models describe the particle mobility in terms of the polymer dynamics,[13,17,18] which are set by the characteristic length scales ξ and the polymer radius of gyration R_g. Identifying the relevant physics requires model systems that are compatible with a wide range of particle sizes and span the transition from dilute to semidilute regimes in unentangled solutions. In polyelectrolyte solutions, topological entanglements appear at concentrations orders of magnitude above c^*,[19,20] enabling investigations of nanoparticle dynamics across a wide and previously inaccessible

range of semidilute concentrations in the absence of entanglements.

Here, we show that the long-time diffusivity of nanoparticles in unentangled semidilute polymer solutions is controlled by R_{NP}/ξ. We measure the mobility of nanoparticles of varying size with $R_{NP} \sim R_g$ over time. On short time scales, particle motion is subdiffusive; on long time scales, particle motion becomes purely diffusive. For large particles the long-time diffusivity agrees with the SE prediction, but as the particle size decreases the particles diffuse faster than predicted. Furthermore, the discrepancy between measured diffusivities and SE predictions increases with decreasing particle radius. To explain these deviations, we use a model that assumes coupling between particle and polymer dynamics to predict a size-dependent diffusivity.[13] This model collapses the long-time particle diffusivities onto a single curve and accurately predicts the scaling of the crossover time between subdiffusive and Fickian dynamics for large particles. For small particles, however, the subdiffusive behavior suggests only partial coupling to polymer dynamics.

Fluorescent polystyrene nanoparticles ranging from 300 nm to 2 μm in diameter (Fluoro-Max, Thermo Fisher Scientific) are suspended in aqueous solutions of partially hydrolyzed polyacrylamide (HPAM) with a weight-averaged molecular weight of 8 000 000 Da and a hydrolysis fraction of ~30% (SNF, FLOPAAM 3330). We select these particle sizes to span
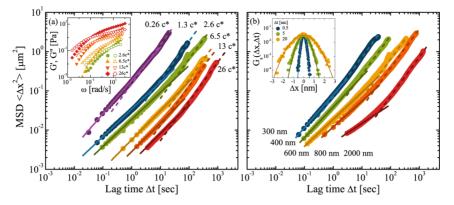
Figure 1. Mean-squared displacement (MSD, $\langle \Delta x^2 \rangle$) as a function of lag time Δt for (a) 600 nm particles in solutions of varying polymer concentration and for (b) particles of varying size in a solution of polymer concentration $2.6c^*$. Dashed lines are linear fits at long time scales, and solid lines are power law fits with a variable exponent. Inset (a) Storage (closed) and loss (open) moduli for solutions of various concentrations. Inset (b) Normalized distribution of particle displacements at various times for 600 nm particles in a solution of polymer concentration $1.3c^*$. Solid lines are Gaussian fits.

R_g and hence probe the crossover to bulk behavior, in contrast to our previous work focusing on a single particle size.[21] Dynamic light scattering measurements confirm that the polymer does not absorb to the surface of the particles. Our solutions are well below the entanglement concentration for polyelectrolyte solutions.[20] We determine the radius of gyration in dilute solutions $R_{g,0}$ = 270 nm from intrinsic viscosity measurements and estimate the overlap concentration $c^* = M_W/(4/3\pi N_{av} R_{g,0}^3) = 0.16$ g/L. The weight fraction of particles varies from 2×10^{-5} to 8.5×10^{-5} for 300 nm and 2 μm particles, respectively, to increase particle tracking statistics while minimizing interparticle interactions. Quiescent samples are imaged using a Leica DM4000 inverted microscope with 40× air and 63× and 100× oil immersion objective lenses. We use particle-tracking algorithms[22] to locate and track the particles over time. From particle trajectories, we calculate the one-dimensional ensemble-averaged mean-squared displacement (MSD) $\langle \Delta x^2(\Delta t) \rangle$ as a function of lag time Δt. We fit the short-time data to a power law $\langle \Delta x^2(\Delta t) \rangle = 2D'(\Delta t)^\alpha$ and the long-time data to $\langle \Delta x^2(\Delta t) \rangle = 2D(\Delta t)$.

The nanoparticle mobility changes as a function of polymer concentration (Figure 1(a)) and nanoparticle size (Figure 1(b)). The particle dynamics are subdiffusive at short time scales and crossover into a Fickian regime at longer times. The crossover times are comparable to the longest relaxation time $\tau \approx 1{-}100$ s of the polymer in solution, estimated from bulk rheology (inset to Figure 1(a)). The distribution of particle displacements remains Gaussian throughout the crossover (inset to Figure 1(b)), indicating that each particle experiences the same homogeneous environment for all accessible lag times with no signs of hopping diffusion. From the long-time slope, we extract the particle diffusivity D and normalize by the diffusivity in pure solvent D_0 to remove explicit size dependence. For large particles, e.g., 2 μm particles in $2.6c^*$ solution, the relative diffusivity agrees with predictions of D_{SE}[21] and does not depend on particle size. By contrast, the relative diffusivity of smaller particles strongly deviates from D_{SE} (Figure 2). Moreover, the ratio of particle diffusivity to the SE prediction D/D_{SE} increases with decreasing particle radius and increasing polymer concentration (inset to Figure 2), indicating that diffusivity depends on both particle and polymer length scales.
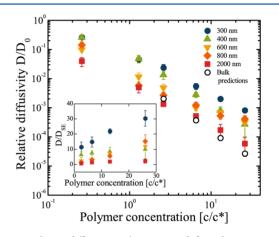

Figure 2. Relative diffusivity D/D_0 extracted from long-time mean-squared displacement as a function of normalized polymer concentration c/c^*. Bulk predictions (open circles) are calculated from the zero-shear viscosity of the bulk polymer solution. (Inset) Ratio between experimental diffusivity and SE prediction D/D_{SE} as a function of c/c^*.

To explain the effects of the characteristic length scales on particle diffusion, models typically use either obstruction or hydrodynamic theories. Obstruction models describe particle diffusion in the limit of small particles and dilute solutions.[23−28] As the probe particles become larger and the polymer concentration increases, however, hydrodynamic interactions become important.[25−27] In hydrodynamic models,[10,15,16] the particle diffusivity D scales as $D/D_0 = \exp(a(L/\xi)^b)$ where L is a function of particle radius R_{NP} and/or R_g.[10,29−32] R_g is a weak function of polymer concentration, scaling as $R_g \approx R_{g,0}(c/c^*)^{-0.15}$, whereas ξ is a much stronger function, scaling as $\xi \approx R_{g,0}(c/c^*)^{-0.71}$.[20,33,34] These scaling relationships slightly deviate from predictions for polymers in good solvents because repulsions between charged groups cause HPAM to adopt a slightly extended configuration. Although these models can fit our data over limited ranges of polymer concentration or particle size, none of these models cleanly collapse the data across the entire range of polymer or particle length scales (see Supporting Information). We now show that coupling between particle and polymer dynamics on long time scales can explain deviations from SE behavior.

The dynamic crossover in the particle MSDs (Figure 1) suggests that the particle dynamics are coupled to those of the polymers because polymers undergo similar crossovers between dynamic modes. In a semidilute unentangled solution, polymers undergo Zimm-like motion over length scales smaller than ξ. The relaxation time of a correlation blob is $\tau_\xi \approx \eta_0 \xi^3 / k_B T$. On longer time scales $t > \tau_\xi$, the polymer moves according to Rouse motion as a chain of correlation blobs. The polymer moves subdiffusively for $\tau_\xi < t < \tau_R \approx \tau_\xi (N/N_\xi)^{2\nu+1}$, where N and N_ξ represent the number of monomers in the polymer chain and a correlation blob, respectively, and ν is the reciprocal of the fractal dimension of the polymer. In semidilute solutions, excluded volume effects are screened over length scales larger than ξ.[35] Thus, the polymer behaves as an ideal string of correlation blobs with $\nu = 1/2$. At τ_R, the polymer fully relaxes and moves diffusively with a Rouse friction coefficient of $\zeta_R \approx \eta_0 \xi N / N_\xi$. Although we cannot access time scales $t < \tau_\xi$ due to resolution and frame rate limitations associated with optical tracking techniques, the subdiffusive behavior of the particles and the crossover into Fickian diffusion mimics the dynamics of the polymer, suggesting that particle and polymer dynamics are coupled.

The mobile polymer chains locally cage the particles until the polymer has sufficient time to relax,[21] resulting in the coupling between particle and polymer dynamics. To quantitatively understand the implications of particle−polymer coupling on particle dynamics, ref 13 extended the scaling model of ref 17 to account for regimes of different particle sizes, summarized here. On very short time scales, the particle does not interact with the polymer and moves diffusively according to solvent viscosity. At $t = \tau_\xi$, the particle begins to interact with correlation blobs of size ξ. For $t > \tau_\xi$, the particle feels the local caging and begins to couple to relaxation modes in the polymer. At a time $t > \tau_\xi$, the particle interacts with a section of a polymer chain with a relaxation time $t \approx \tau_\xi (N/N_\xi)^2$. As time increases, larger sections of the polymer relax and interact with the particle, so that the effective viscosity felt by the particle increases as $\eta_{eff}(t) \sim N(t)/N_\xi \approx \eta_0 (t/\tau_\xi)^{1/2}$. The viscosity will continue to increase until the polymer relaxes over the size of the particle; at this time $\tau_R \approx \tau_\xi (2R_{NP}/\xi)^4$, the particle and polymer dynamics decouple. Thereafter, the long-time dynamics of the particles depend on the effective viscosity $\eta_{eff}(\tau_R) \approx \eta_0 (2R_{NP}/\xi)^2$.

We compare the long-time diffusivity of the particles to predictions from ref 13 using η_{eff} and the SE equation. The relative diffusivities D/D_0 collapse onto a single curve for particles ranging from 300 to 800 nm in diameter (Figure 3). The data are consistent with the predicted scaling of $D/D_0 \sim (2R_{NP}/\xi)^{-2}$. The larger 2 μm particles lie somewhat off of the curve because they are large enough to experience the viscoelasticity of the bulk solution. This can be seen by normalizing the particle diffusivities by $D_{SE} \sim (\eta_{bulk} R_{NP})^{-1}$. The bulk viscosity scales with concentration as $\eta_{bulk} \sim (c/c^*)^{1.95}$, which deviates from predictions for semidilute unentangled solutions.[20,35] After combining the concentration dependencies of the bulk viscosity and correlation length, the normalized diffusivities are predicted to scale as $D/D_{SE} \sim (R_{g,0}/R_{NP})^2 (c/c^*)^{0.53}$. The concentration dependence is unique to aqueous solutions of HPAM due to bulk viscosity scaling (see Supporting Information). For the smaller particles, the normalized diffusivities D/D_{SE} closely follow this predicted scaling (inset to Figure 3). When the particles are sufficiently large, they experience bulk viscosity and $D \approx D_{SE}$. The
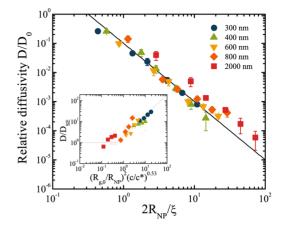

Figure 3. Relative diffusivity D/D_0 as a function of particle to polymer size ratio $2R_{NP}/\xi$. Solid line is the predicted scaling.[13] (Inset) Ratio between experimental diffusivity and SE prediction D/D_{SE} as a function of particle size and bulk viscosity scaling for HPAM. Solid line represents predicted scaling behavior.[13]

crossover to bulk behavior for long-time diffusivity occurs when $R_{NP} \approx R_{g,0}$, in good agreement with theory and simulations.[13,36−38]

The collapse of the long-time dynamics onto a single scaling curve confirms that the particle interacts on long time scales with comparably sized sections of polymer. Ref 13 predicts that these interactions arise from coupling between particle dynamics and polymer relaxation modes on short time scales. We therefore examine the scaling behavior of the particle dynamics in the subdiffusive regime. We estimate the predicted scaling for particle MSDs in the subdiffusive regime from $\langle \Delta x^2 \rangle \sim D(\Delta t) \Delta t$ where $D(\Delta t) \sim 1/R_{NP} \eta_{eff}(\Delta t)$. Therefore, the MSDs of the particles should scale with time as $\langle \Delta x^2 \rangle \sim (\Delta t)^{1/2}$.

The particles exhibit subdiffusive behavior for most particle sizes and polymer concentrations, characterized by the subdiffusive exponent α (Figure 4(a)). For 300 and 400 nm particles in solutions with $c < c^*$ the short time behavior is largely diffusive because $R_{NP} < \xi$. As the particle size and polymer concentration increase, the subdiffusive exponents decrease, reaching $\alpha \approx 0.5$ for the largest 2 μm particles. This subdiffusive behavior persists for at least one decade in time with constant α; at intermediate polymer concentrations, it persists for up to three decades. The surprising persistence of the subdiffusive dynamics with constant α suggests that the subdiffusive regime is not solely due to crossover between two Fickian regimes. The higher-than-predicted subdiffusive exponents indicate that the particle dynamics are not directly coupled to the relaxation modes of the polymer even when $R_{NP} \gg \xi$. Coupling on short time scales is only seen for the largest 2 μm particles in solutions of concentration $c > c^*$ despite even the smallest particles being over an order of magnitude larger than ξ. Additionally, the crossover time τ_c between subdiffusive and Fickian regimes is predicted to occur at $\tau_c \approx \tau_R \sim R_{NP}^4 \xi^{-1}$. When the particles are coupled to the polymer, i.e., the 2 μm particles with $\alpha \approx 0.5$, the crossover time scales as predicted (Figure 4(b)). When the particles deviate from polymer relaxation modes at short times ($\alpha > 0.5$), the crossover times are larger than predicted and clearly cannot be collapsed onto the scaling prediction. The dependence of the subdiffusive exponent on particle size and polymer concentration and the lack of agreement between crossover time and predicted scaling
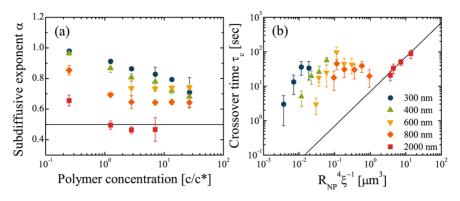
Figure 4. (a) Subdiffusive exponent α as a function of normalized polymer concentration c/c^*. Solid line corresponds to $\alpha = 0.5$. (b) Crossover time τ_c as a function of particle and polymer length scales. Solid line represents predicted scaling behavior.[13]

imply that the particles are not directly coupled to the relaxation modes of the polymer on short time scales. Moreover, the deviations increase as the particle size or polymer concentration is decreased, consistent with the idea that the confinement becomes softer as the particle size decreases. Nonetheless, the partial coupling on short time scales does not persist to long times; the excellent agreement for the long-time diffusivities indicates that particle dynamics depends on interactions between particles and comparably sized sections of polymer.

The long-time diffusivity of particles in semidilute unentangled solutions of polymers depends on the interaction of the particle with sections of polymer of comparable size. As a result, the diffusivity of nanoparticles depends on the particle size when $R_{NP} < R_g$ and is independent of particle size when $R_{NP} \geq R_g$. The long-time particle diffusivities collapse onto a single curve as a function of R_{NP}/ξ, and the soft confinement on short time scales does not impact this scaling. Notably, this collapse suggests that length scales such as ξ can be obtained from simple diffusion experiments. For polymer systems in which the variation in correlation length and size is known from independent measurements or scaling arguments, these measurements can be used to infer local structure and deformation state. For soft matter systems in which these length scales are not known a priori, mobility experiments with an appropriate choice of probes may enable efficient measurements of structural properties of a wide range of complex media, including cellular cytoplasm,[30] nucleic fluid,[39] suspensions of rigid rods,[40] and emulsions.[41]

ASSOCIATED CONTENT

ⓈSupporting Information

The Supporting Information is available free of charge on the ACS Publications website at DOI: 10.1021/acsmacrolett.5b00616.

> Detailed description of experimental methods, dynamic light scattering results, intrinsic viscosity measurements, polymer properties, and diffusivity plots for different hydrodynamic models (PDF)

AUTHOR INFORMATION

Corresponding Authors
*E-mail: ramanan@uh.edu.
*E-mail: jcconrad@uh.edu.

Notes
The authors declare no competing financial interest.

REFERENCES

(1) Peer, D.; Karp, J. M.; Hong, S.; Farokhzad, O. C.; Margalit, R.; Langer, R. *Nat. Nanotechnol.* **2007**, *2*, 751−760.
(2) Tang, L.; et al. *Proc. Natl. Acad. Sci. U. S. A.* **2014**, *111*, 15344−15349.
(3) Lin, Y.; Skaff, H.; Emrick, T.; Dinsmore, A. D.; Russell, T. P. *Science* **2003**, *299*, 226−229.
(4) Bresme, F.; Oettel, M. *J. Phys.: Condens. Matter* **2007**, *19*, 413101.
(5) Winey, K. I.; Vaia, R. A. *MRS Bull.* **2007**, *32*, 314−358.
(6) Kashiwagi, T.; Du, F.; Douglas, J. F.; Winey, K. I.; Harris, R. H.; Shields, J. R. *Nat. Mater.* **2005**, *4*, 928−933.
(7) Mackay, M. E.; Dao, T. T.; Tuteja, A.; Ho, D. L.; van Horn, B.; Kim, H.-C.; Hawker, C. J. *Nat. Mater.* **2003**, *2*, 762−766.
(8) Tuteja, A.; Mackay, M. E.; Narayanan, S.; Asokan, S.; Wong, M. S. *Nano Lett.* **2007**, *7*, 1276−81.
(9) Ye, X.; Tong, P.; Fetters, L. J. *Macromolecules* **1998**, *31*, 5785−5793.
(10) Cheng, Y.; Prud'homme, R. K.; Thomas, J. L. *Macromolecules* **2002**, *35*, 8111−8121.
(11) Kalathi, J. T.; Yamamoto, U.; Schweizer, K. S.; Grest, G. S.; Kumar, S. K. *Phys. Rev. Lett.* **2014**, *112*, 108301.
(12) Yamamoto, U.; Schweizer, K. S. *Macromolecules* **2015**, *48*, 152−163.
(13) Cai, L.-H.; Panyukov, S.; Rubinstein, M. *Macromolecules* **2011**, *44*, 7853−7863.
(14) Guo, H.; Bourret, G.; Lennox, R. B.; Sutton, M.; Harden, J. L.; Leheny, R. L. *Phys. Rev. Lett.* **2012**, *109*, 055901.
(15) Cukier, R. I. *Macromolecules* **1984**, *17*, 252−255.
(16) Phillies, G. D. J.; Ullmann, G. S.; Ullmann, K.; Lin, T.-H. *J. Chem. Phys.* **1985**, *82*, 5242.
(17) Brochard Wyart, F.; de Gennes, P. *Eur. Phys. J. E: Soft Matter Biol. Phys.* **2000**, *1*, 93−97.
(18) Cai, L.-H.; Panyukov, S.; Rubinstein, M. *Macromolecules* **2015**, *48*, 847−862.
(19) Boris, D. C.; Colby, R. H. *Macromolecules* **1998**, *31*, 5746−5755.
(20) Colby, R. H. *Rheol. Acta* **2010**, *49*, 425−442.
(21) Babaye Khorasani, F.; Poling-Skutvik, R.; Krishnamoorti, R.; Conrad, J. C. *Macromolecules* **2014**, *47*, 5328.
(22) Crocker, J.; Grier, D. G. *J. Colloid Interface Sci.* **1996**, *179*, 298−310.

(23) Mackie, J. S.; Meares, P. *Proc. R. Soc. London, Ser. A* **1955**, *232*, 510−518.

(24) Ogston, A. G. *Trans. Faraday Soc.* **1958**, *54*, 1754.

(25) Ogston, A. G.; Preston, B. N.; Wells, J. D. *Proc. R. Soc. London, Ser. A* **1973**, *333*, 297−316.

(26) Mustafa, M. B.; Tipton, D. L.; Barkley, M. D.; Russo, P. S.; Blum, F. D. *Macromolecules* **1993**, *26*, 370−378.

(27) Waggoner, R. A.; Blum, F. D.; MacElroy, J. M. D. *Macromolecules* **1993**, *26*, 6841−6848.

(28) Amsden, B. *Macromolecules* **1999**, *32*, 874−879.

(29) Hołyst, R.; Bielejewska, A.; Szymański, J.; Wilk, A.; Patkowski, A.; Gapiński, J.; Zywociński, A.; Kalwarczyk, T.; Kalwarczyk, E.; Tabaka, M.; Ziebacz, N.; Wieczorek, S. A. *Phys. Chem. Chem. Phys.* **2009**, *11*, 9025−32.

(30) Kalwarczyk, T.; Ziębacz, N.; Bielejewska, A.; Zaboklicka, E.; Koynov, K.; Szymański, J.; Wilk, A.; Patkowski, A.; Gapiński, J.; Butt, H. J.; Hołyst, R. *Nano Lett.* **2011**, *11*, 2157−2163.

(31) Ziębacz, N.; Wieczorek, S. A.; Kalwarczyk, T.; Fiałkowski, M.; Hołyst, R. *Soft Matter* **2011**, *7*, 7181.

(32) Kohli, I.; Mukhopadhyay, A. *Macromolecules* **2012**, *45*, 6143−6149.

(33) Takahashi, A.; Nagasawa, M. *J. Am. Chem. Soc.* **1964**, *86*, 543−548.

(34) Noda, I.; Tsuge, T.; Nagasawa, M. *J. Phys. Chem.* **1970**, *74*, 710−719.

(35) Rubinstein, M.; Colby, R. H. *Polymer Physics*; Oxford University Press: New York, 2003.

(36) Ganesan, V.; Pryamitsyn, V.; Surve, M.; Narayanan, B. *J. Chem. Phys.* **2006**, *124*, 221102.

(37) Liu, J.; Cao, D.; Zhang, L. *J. Phys. Chem. C* **2008**, *112*, 6653−6661.

(38) Yamamoto, U.; Schweizer, K. S. *J. Chem. Phys.* **2011**, *135*, 224902.

(39) Lukacs, G. L.; Haggie, P.; Seksek, O.; Lechardeur, D.; Freedman, N.; Verkman, A. S. *J. Biol. Chem.* **2000**, *275*, 1625−1629.

(40) Pryamitsyn, V.; Ganesan, V. *Phys. Rev. Lett.* **2008**, *100*, 128302.

(41) Clara-Rahola, J.; Brzinski, T. A.; Semwogerere, D.; Feitosa, K.; Crocker, J. C.; Sato, J.; Breedveld, V.; Weeks, E. R. *Phys. Rev. E* **2015**, *91*, 010301(R).